Effects of Multiple Scattering on Rocket Exhaust Plume Smoke Visibility

A. C. Victor*
U.S. Naval Weapons Center, China Lake, California

An approximate method of solution for the scattering of radiation by optically thick media is described. Multiple scattering functions, analogous to single scattering functions, are derived by a Monte Carlo technique. For a given particle size distribution, these multiple scattering functions are related only to the single scattering function and the optical depth. For cases such as combustion smoke in which the particle number density varies but the particle size distribution is fairly constant, a straightforward method is given for interpreting light scattering data and for predicting light scattering or visibility. For the cases described in this paper, scattering by alumina particle clouds with optical depths of 0.2–10, the multiple scattering functions differ greatly from the single scattering function only in the forward direction. In other directions, the two functions agree within a factor of 4. The differences would be much greater for nonabsorbing particles. The results are compared to earlier rocket exhaust smoke visibility calculations that presumed single scattering. For an optical depth of <0.5, a single scattering computation is adequate. Lambert law reflection is an extreme assumption corresponding to optical depths significantly >10.

Nomenclature

a = particle radius, m
d = diameter [Eq. (4)]
F = scattering function
i = Mie function
ℓ = distance from scattering particle to detector, m
L = distance light packet travels between interactions with particles, m
LP = light packet; may be considered to be a photon
n = particle concentration, m^{-3}
PR_1 = probability that light packet particle interaction occurs at length L into the scattering volume
PR_2 = probability that particle involved in the interaction is of radius r
PR_3 = probability that light packet is absorbed
PR_4 = probability that scattering angle is θ_s in ξ-ζ plane, based on single-scattering Mie functions for the particle distribution
PR_5 = probability that scattering angle is ϕ_s in ξ-η plane, based on single-scattering Mie functions for the particle distribution
Q_{abs} = absorption coefficient, single particle
Q_{ext} = extinction coefficient, single particle
r = radius of specific particle, m
$\bar{r}$ = radius of "average" particle
r_μ = radius of specific particle, μm [Eq. (3)]
x,y,z = Cartesian coordinates of particle-containing sphere, with initial LP vector along z
α = multiple scattering factor [Eqs. (1) and (2)]
ζ,η,ξ = Cartesian coordinates of LP-particle interaction, with ξ-ζ plane parallel to z axis
θ = scattering angle in ξ-ζ plane
λ = wave length of radiation, m
τ = optical depth [Eq. (4)]; this is the exponential term in the Beer-Lambert transmission-attenuation equation
ϕ = scattering angle in ξ-η plane

Subscripts

i = incident
K = index referring to particles of a specific radius r_K
ms = multiple scattering
o = original (a special case of incidence)
s = scattered
ss = single scattering

Received May 9, 1988; revision received Nov. 21, 1988. This paper is declared a work of the U.S. Government and is not subject to copyright protection in the United States.

*Physicist, Ordnance Systems Department. Associate Fellow AIAA.

Introduction

An earlier paper described a method for calculating the visibility of smokey rocket exhaust plumes, assuming single scattering by a polydispersion of small alumina particles.[1] The current study is directed toward expanding the single scattering method to optically thick plumes that require multiple scattering calculations.

Many authors have described methods for computing multiple scattering (or "radiative transfer"). All of these methods suffer from one or more of the following shortcomings: mathematical complexity, inaccuracy, conceptual obscurity, or long computation times.[2-5]

The solution of a number of practical problems would be simplified if the multiple scattering problem could be shaped into the form of the single scattering function. This would be particularly useful for cases in which the particle size distribution is invariant despite variations in particle number density. Many combustion smokes fall into this category. Unfortunately fog, clouds, haze, and condensation contrails have fairly complex variations in both particle size and number density distribution, which would decrease the usefulness of such an approach.

Monte Carlo techniques for calculating multiple scattering are well known and conceptually very simple. The major disadvantage of these techniques is the long computation times required if many different problems are to be solved. However, in certain problems enough variables remain constant that the results of a few Monte Carlo calculations may be saved and reused even though other parameters of the problem change. One example of this involves combustion smoke for which the particle size distribution remains fairly constant

despite large variations in smoke concentration. For such cases one would expect the angular distribution of multiply scattered light emerging from smoke clouds to be a function of cloud shape and optical depth, and independent of cloud dimensions.

A further refinement can easily be envisioned, although it is not pursued in this study. If the elemental multiple scattering cloud is conceived as a sphere, then the calculation of radiative transfer between a few such spheres should be a reasonable way of simulating the multiple scattering effects of an irregularly shaped volume.

The technique described in this paper was developed to predict the effects of multiple scattering in rocket exhausts containing alumina particles, the subject of the earlier paper (Ref. 1).

Initially it was the author's intention simply to use Monte Carlo calculations to assess the importance of multiple vs single scattering in these exhausts. However, it quickly became obvious that if one assumed a spherical shape for the scattering volume (V) and forced every light packet (LP) to pass along a diameter of the sphere, the sphere would in effect enclose nV particles, each of which scattered identically but with a scattering function determined by the single scattering Mie function of all the different-size particles in the volume, the particle size distribution, and the number of particles in the volume. Since an effective single scattering function could be (and in fact previously had been) written for such a volume,[1] obviously a similar multiple scattering function could also be defined. It was simply a matter of normalizing the multiple scattering function to a base comparable to that used for the single scattering function.

Multiple Scattering Calculation

The beauty of the Monte Carlo method for multiple scattering calculations lies in its simplicity. In using this method individual LP's are traced in a computer code as they interact with particles in the volume under study. Whenever an interaction occurs, the result is computed probabilistically. The LP is traced through all its interactions until it leaves the volume either by absorption or by being scattered out. The logic flow of the scattering calculation is shown in Fig. 1.

The geometry of the generalized scattering interactions is shown in Fig. 2. The x, y, z coordinate system is determined by the problem geometry in such a way that the original source is at $z = -\infty$ and the origin is at the center of the volume under consideration (a sphere of radius R_o). For any scattering, the LP is assumed to be traveling in the direction θ_i, ϕ_i and to have traversed a distance L from the previous scattering location x_1, y_1, z_1. (For the initial case, $x_1 = y_1 = 0$, $z_1 = -R_o$, $\theta_i = 0$, $\phi_i = 0$.) The new scattering center is at

$$x_2 = x_1 + L \sin\theta_i \cos\phi_i$$

$$y_2 = y_1 + L \sin\theta_i \sin\phi_i$$

$$z_2 = z_1 + L \cos\theta_i$$

If this point lies within the defined volume ($x_2^2 + y_2^2 + z_2^2 \leq r_o^2$), the LP scatters in a direction θ_s, ϕ_s with respect to its previous line of motion (ζ axis in Fig. 2). The symmetry of the scattering permits flexibility in the choice of the ξ axis; for convenience, the ξ-ζ plane is chosen to be parallel to the z axis. The new direction of motion (θ_o, ϕ_o) for the LP with respect to the fixed axes is then given by

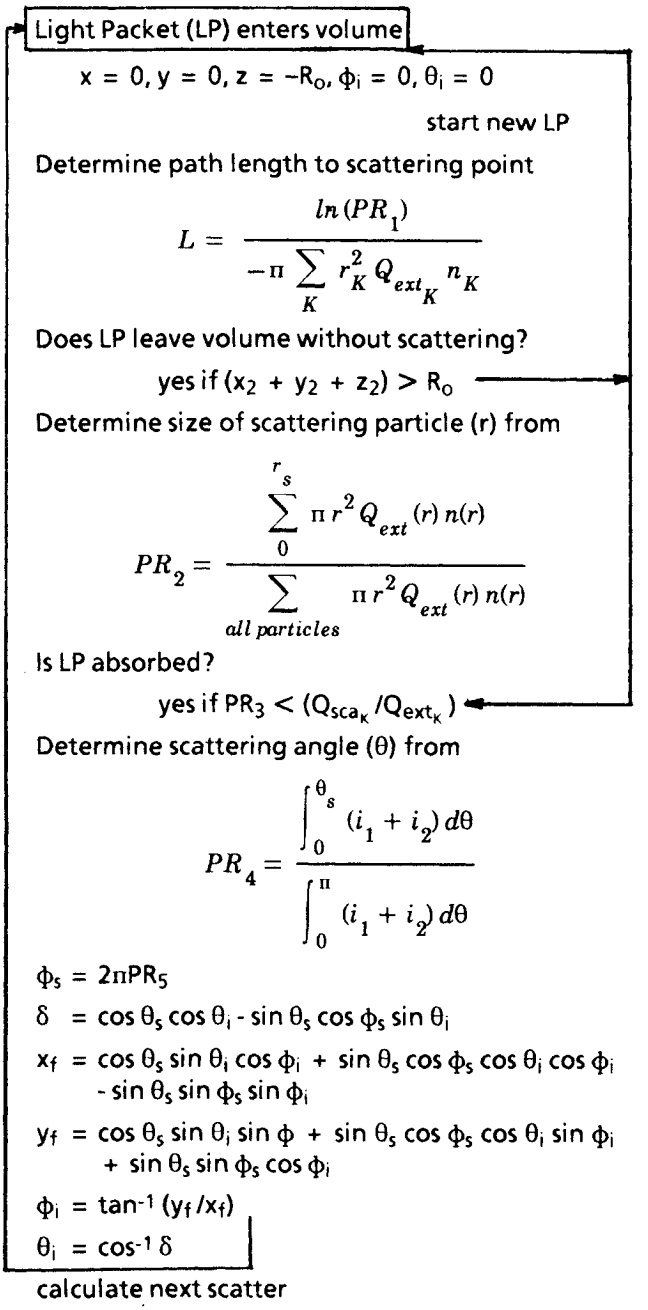

Fig. 1 Flowchart of Monte Carlo multiple scattering calculation.

The values are then updated; θ_i is set equal to θ_o, ϕ_i to ϕ_o, x_1 to x_2, etc.; a new value for L is obtained, and the next scattering is treated.

Multiple Scattering Functions

The value of the single scattering function at any angle is proportional to the scattered energy at that angle divided by the energy incident on the particle. The same proportionality must hold for multiple scattering functions. The values of the multiple scattering functions are calculated after an entire Monte Carlo run has been made and the number of light packets is known.

$$\cos\theta_o = \cos\theta_s \cos\theta_i - \sin\theta_s \cos\phi_s \sin\theta_i$$

$$\tan\phi_o = \frac{\cos\theta_s \sin\theta_i \sin\phi_i + \sin\theta_s \cos\phi_s \cos\theta_i \sin\phi_i + \sin\theta_s \sin\phi_s \cos\phi_i}{\cos\theta_s \sin\theta_i \cos\phi_i + \sin\theta_s \cos\phi_s \cos\theta_i \cos\phi_i - \sin\theta_s \sin\phi_s \sin\phi_i}$$

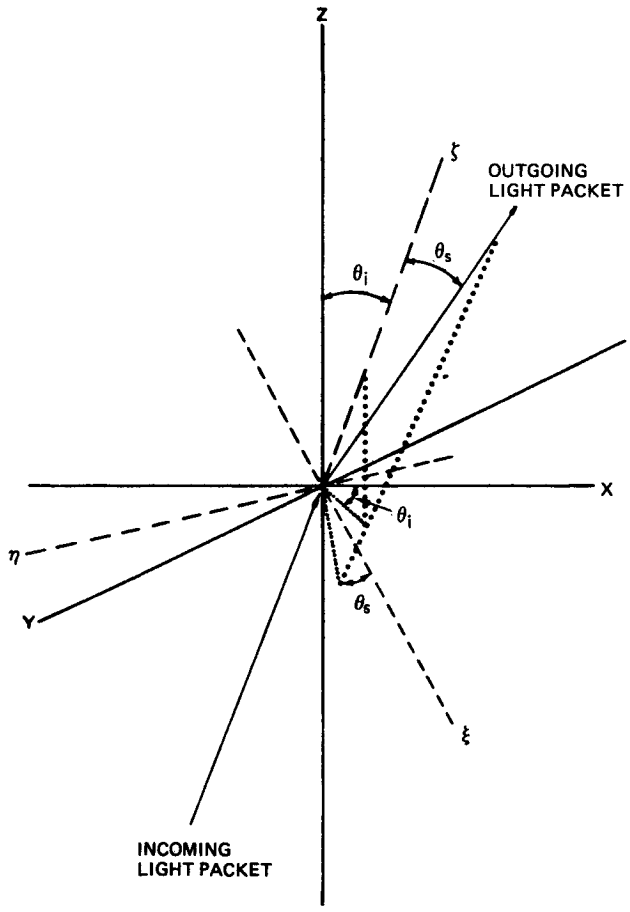

Fig. 2 Geometry of scattering interactions.

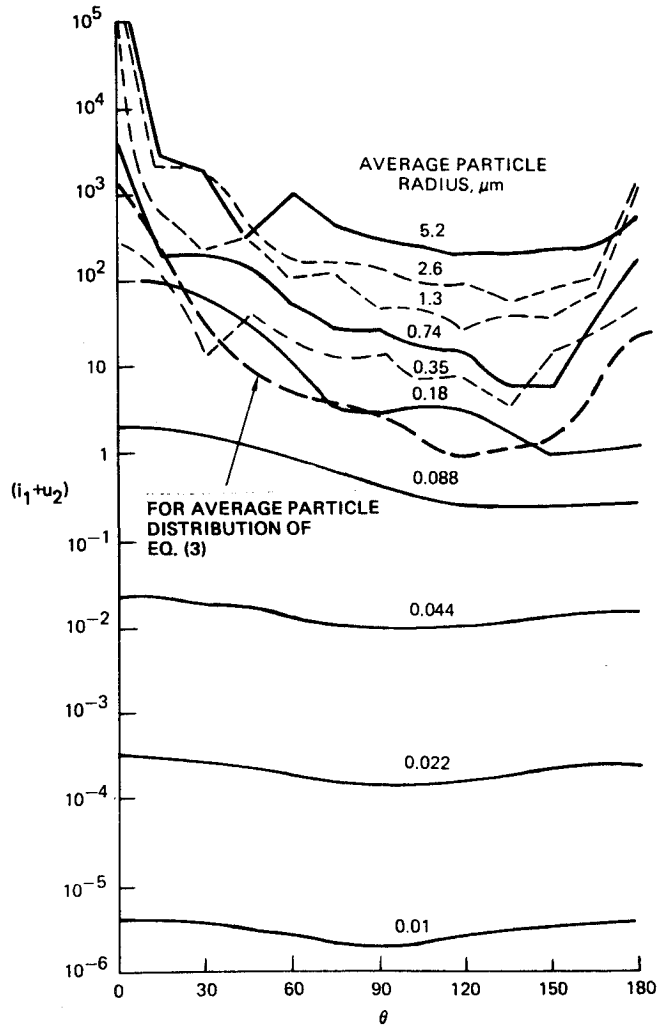

Fig. 3 Calculated Mie functions for Al_2O_3 particles with refractive index $m = 1.71-0.01i$ for $\lambda = 0.55$ μm (from Ref. 5).

Input for the multiple scattering computer code consists of particle radius r_K, particle number density n_K, extinction coefficient Q_{ext_K}, absorption coefficient Q_{abs_K}, and values of the single scattering Mie coefficients $(i_1 + i_2)_{K_i}$ for a number of angles sufficient to construct a curve of the Mie function. The same information is needed for every particle size chosen to represent the homogeneous distribution in the scattering distribution. The single scattering Mie coefficients and absorption and extinction coefficients are generated by a separate code. Additional input consists of the diameter of the spherical scattering volume and the number of light packets to be used for each individual problem analysis.

The average single scattering optical properties of the volume can be summarized as follows:

$$\bar{r} = \left(\sum_K n_K r_K^2 \Big/ \sum_K n_K\right)^{1/2}$$

$$\bar{Q}_{\text{ext}} = \sum_K n_K Q_{\text{ext}_K} r_K^2 \Big/ \sum_K n_K r_K^2$$

$$(\bar{Q}_{\text{abs}})_{\text{ss}} = \sum_K n_K Q_{\text{abs}_K} r_K^2 \Big/ \sum_K n_K r_K^2$$

The values of $\bar{r}$ and $\bar{Q}_{\text{ext}}$ will also apply to the multiple scattering problem. However, because the probability of absorption increases with the number of interactions, the absorption coefficient will be larger for multiple scattering problems.

$$(\bar{Q}_{\text{abs}})_{\text{ms}} = \bar{Q}_{\text{ext}}\left(\frac{\text{number of LP's absorbed}}{\text{number of LP} - \text{particle interactions}}\right)$$

The multiple scattering function $F_{\text{ms}}(\theta)$ is given by

$$F_{\text{ms}}(\theta) = a(\theta)[i_1(\theta) + i_2(\theta)] \tag{1}$$

where

$$a(\theta) = \frac{\left(\dfrac{\text{number of LP's scattered at } \theta}{\text{total number of LP interactions}}\right)}{\dfrac{[i_1(\theta) + i_2(\theta)]}{\dfrac{\Sigma n_K \int [i_1(\theta) + i_2(\theta)]_K d\theta}{\Sigma n_K}}} \tag{2}$$

For a scattering substance in which the particle size distribution remains the same despite changes in the particle concentration, $a(\theta)$ will vary as a function of the optical depth of the scattering medium. This is shown for a particular case in the next section.

Sample Case

The case examined here involves scattering of visible light ($\lambda = 0.55$ μm) by an exhaust dispersion typical of aluminized rocket motor propellants (containing aluminum oxide). The particle size distribution is given by Eq. (3) (taken from Ref. 1) for particles-m^{-3} at a density equivalent to 1% aluminum

Table 1 Properties of scattering particles for $\lambda = 0.55$ μm

Radius, μm	No. density,[a] m^{-3}	Q_{ext}	Q_{abs}
5.6	1.8 (5)[b]	1.06	0.434
2.8	1.2 (9)	1.07	0.369
1.4	4.8 (10)	1.24	0.268
0.70	1.24 (11)	1.43	0.189
0.35	1.13 (11)	1.74	0.115
0.18	4.75 (11)	1.51	0.0465
0.088	9.3 (11)	0.225	0.0146
0.044	6.1 (11)	0.0184	0.0051
0.022	1.7 (11)	0.0030	0.0022
0.011	2.6 (10)	0.0012	0.0011

[a]Per 1% alumina by weight in volume. [b]Numbers in parentheses represent powers of 10.

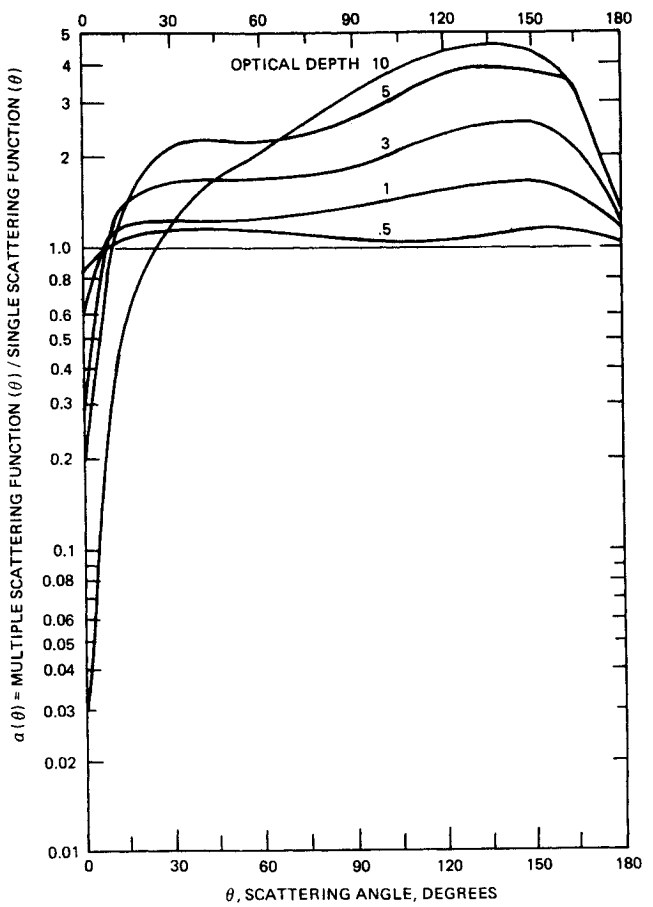

Fig. 4 Dependence of multiple scattering on optical depth.

oxide by weight suspended uniformly in the exhaust gas. Spherical particles were assumed in all calculations.

$$n_K(r) = 1.11 \times 10^{22} r_\mu^4 \exp(-35.9 r_\mu^{0.5}) + 5.33 \times 10^{13} r_\mu^3 \exp(-6 r_\mu) \quad (3)$$

The single scattering Mie functions for the important size particles in this distribution are shown in Fig. 3.

Table 1 summarizes the properties of the particles. All calculations were made for spheres of 1-m-diam with the optical depth varying from 0.02–10.0.

$$\tau = \left(\sum_K n_K \pi r_K^2 Q_{ext_K} \right) d \quad (4)$$

The results of the calculations are shown in Fig. 4 as curves of $a(\theta)$ vs θ for five values of optical depth. The value at any angle was smoothed by the computer code if the value at that angle corresponded to less than 2% of the total scattered radiation. Since the multiple scattering curve for an optical depth of 0.5 is within 20% of the single scattering curve at all points, it may be safely assumed that single scattering calculations are usually sufficiently accurate for lower values of optical depth.

The function of $a(\theta)$ in Fig. 4 follows the form of orthogonal polynomials known as Gegenbauer (ultraspherical) polynomials,[6-8] $C_n^{(\beta)}(x)$, as given in Eq. (5).

$$a(\theta) \simeq \exp[C_n^{(\beta)}(x)] \quad (5)$$

where $x = 0.0025\theta - 1$; θ = scattering angle, deg; $\beta = \tau/10$; and $n \simeq 5$.

Solution of Eq. (4) for the parameters in Table 1 gives an optical depth of 0.96 for a 1-m path length (d). (Because of the specific particle size distribution used in this case, only particles with radii between 2.8 and 0.18 μm are important in the solution.) This result may be interpreted to indicate that the curve for an optical depth of 0.5 in Fig. 4 applies to a 1 m sphere of exhaust gas containing 0.52 weight percent of alumina particles. By the same interpretation, the curve for an optical depth of 10 applies to a sphere of gas containing 10.4 weight percent of alumina particles.

Discussion and Conclusions

The results of this study have direct applicability to the results of Ref. 1. In the earlier paper it was assumed that single scattering applied up to a limit, above which Lambert law reflection was assumed to apply [Eqs. (20) and (21) of Ref. 1]. Comparison of angle-dependent Lambert scattering values in Fig. 7 of Ref. 1 with Fig. 4 here shows that Lambert law reflection is an extreme assumption corresponding to optical depths significantly greater than 10.

The general effect of multiple scattering, as determined in this study, can be compared with absolute calculations of single scattering in the earlier paper to arrive at the following generalizations for application to plume visibility predictions.

1) The total radiation scattered by the plume is not substantially changed for moderate-size rocket exhaust plumes.

2) The most notable effect of multiple scattering is to flatten the prominent angle-dependent irregularities in the single scattering curve.

3) Optically dense plume visibility from forward scattering may be substantially lower than single scattering calculations predict.

4) Optically dense plume visibility from back scattering is close to the same predicted by single scattering calculations.

5) For large values of optical depth, multiple scattering increases the plume signature most for scattering angles of 60–170 deg. Since this is the angle range for which single scattering values are lowest, the net effect on overall plume visibility is not substantial.

For the conditions of rocket exhaust gas containing 40 weight percent alumina at the nozzle (close to the upper limit for metalized composite rocket propellants), the optical depth of a 1-m-diam plume will be greater than 0.5 only where the jet has not been diluted by air to an extent of 77 times or more (dilution value of 0.013 or less). According to Eqs. (2-5) of Ref. 1, this condition can occur at sea level for rocket motors with thrusts of 8 kN (1800 lb) or more. For such motors, this

condition will exist for substantial lengths of the plume flowfield only for missiles moving at speeds in excess of Mach 2. For slower moving missiles, the dilution value drops rapidly with plume length, and nontrivial values of optical depth will persist for relatively short lengths.

The optical depth, as derived here, is proportional to the propellant aluminum concentration and to the square root of the rocket motor thrust, which determines the optical path length (nominally 1 m in the preceding plume example). Therefore, it is easy to see that plumes of larger motors, particularly those moving at speeds in excess of Mach 2, will have persistent higher optical depths. The same calculational conditions as above for a rocket motor thrust of 285 kN (64,000 lb) lead to an optical depth of 3.

Some errors are bound to arise when these simple calculations based on spherical multiple scattering results are applied to long, thin plumes. For example, the optical depth at orientations other than broadside to the plume will be larger than broadside values; this will lead to different scattering behavior from that indicated for spherical geometries in Fig. 4. For some scattering angles, the plume shape will cause multiple scattering effects to predominate in certain directions. However, the aforementioned general conclusions are not likely to be seriously wrong.

The calculational method described in this paper can be used in a similar manner for other combustion smokes. (Its greatest advantage is realized for situations in which a common particle size distribution can be applied over a wide range of conditions, and thus avoid repetition of the Monte Carlo computation.) Such situations should exist for a number of stack smokes and fires (industrial, agricultural, and accidental).

The Monte Carlo computation can also be used for vapor condensation fogs, clouds, contrails, and the like. However, since particle distributions in these "smokes" have strong dependencies on ambient conditions, it is not likely that it will be possible to avoid repeating the computation for each separate case studied.

The boundary conditions for spherical geometry and single axis LP source adopted as simplifications in this paper can be replaced readily by specific three-dimensional geometries to adapt the computational method to arbitrary smoke cloud shapes.

Acknowledgment

This work was performed in support of the U.S. Navy's Air-Launched Weaponry Block NW1A, Tactical Missile Propulsion Exploratory Development Program.

References

[1]Victor, A. C. and Breil, S. H., "A Simple Method for Predicting Rocket Exhaust Smoke Visibility," *Journal of Spacecraft and Rockets,* Vol. 14, Sept. 1977, pp. 526–533.

[2]Ludwig, C. B., Malkmus, W., Walker, G. N., Reed, R., and Slack, M., "Standardized Infrared Radiation Model," AIAA Paper 81-1051, 1981.

[3]Chu, C.-M. and Churchill, S. W., "Numerical Solution of Problems in Multiple Scattering of Electromagnetic Radiation," *Journal of Chemical Physics,* Vol. 59, Sept. 1955, pp. 855–863.

[4]Mudgett, P. S. and Richards, L. W., "Multiple Scattering Calculations for Technology," *Applied Optics,* Vol. 10, July 1971, pp. 1485–1502.

[5]Yuen, W. W. and Dunaway, W., "Effect of Multiple Scattering on Radiation Transmission in Absorbing-Scattering Media," *Journal of Thermophysics and Heat Transfer,* Vol. 1, Jan. 1987, pp. 77–82.

[6]Abramowitz, M. and Stegun, I. A., *Handbook of Mathematical Functions,* National Bureau of Standards, Applied Mathematics Series 55, U.S. Government Printing Office, Washington, DC, 1964, p. 777.

[7]Morse, P. M. and Feshbach, H., *Methods of Theoretical Physics,* Part I, McGraw-Hill, New York, 1953.

[8]Bateman, H., *Higher Transcendental Functions,* McGraw-Hill, New York, 1953.